

The Molecular Gas in the Circumnuclear Region of Seyfert Galaxies¹

E. Schinnerer, A. Eckart, L.J. Tacconi
Max-Planck-Institut für extraterrestrische Physik, 85740 Garching, Germany

Received _____; accepted _____

arXiv:astro-ph/9907382v1 27 Jul 1999

¹Based on observations carried out with the IRAM Plateau de Bure Interferometer. IRAM is supported by INSU/CNRS (France), MPG (Germany) and IGN (Spain).

ABSTRACT

Sub-arcsecond IRAM Plateau de Bure mm-interferometric observations of the ^{12}CO (2-1) line emission in the Seyfert 1 NGC 3227 and the Seyfert 2 NGC 1068 have revealed complex kinematic systems in the inner 100 pc to 300 pc that are not consistent with pure circular motion in the host galaxies. Modeling of these kinematic systems with elliptical orbits in the plane of the host galaxy (representing gas motion in a bar potential) is a possible solution but does not reproduce all features observed. A better description of the complex kinematics is achieved by circular orbits which are tilted out of the plane of the host galaxy. This could indicate that the thin circumnuclear gas disk is warped. In the case of NGC 1068 the warp model suggests that at a radius of ~ 70 pc, the gas disk is oriented edge-on providing material for the obscuration of the AGN nucleus. The position-velocity diagrams show rising rotation curves at $r \leq 13$ pc and an indication for large enclosed masses of $\geq 2 \times 10^7 M_{\odot}$ for NGC 3227 and $\geq 10^8 M_{\odot}$ for NGC 1068 within the central 25 pc.

Subject headings: galaxies: ISM - galaxies: nuclei - galaxies: Seyfert - radio lines: ISM - galaxies: individual (NGC 3227) - galaxies: individual (NGC 1068)

1. INTRODUCTION

Molecular gas in the circumnuclear regions of nearby Seyfert galaxies can now be studied via mm-interferometry at sub-arcsecond resolution and high sensitivity. In the standard unified scheme a torus of dense molecular gas and dust surrounding the AGN and its accretion disk (see Peterson 1997 for an overview) is responsible for determining whether the source is seen as a Seyfert 1 or Seyfert 2 depending only on whether the viewing angle onto the central engine is blocked by the torus or not.

Two questions which can be addressed by mm-interferometric observations arise from this picture: (1) On which scales and how much is the molecular gas contributing to the obscuration? (2) What is the transport mechanism which brings the molecular gas down to the AGN?

We have chosen NGC 3227 and NGC 1068 as representative Seyfert 1 and Seyfert 2 templates to address these issues through a detailed analysis of the molecular gas. An extensive description of the results for both sources will be given in two forthcoming papers (Schinnerer et al. 1999 and Schinnerer, Eckart, Tacconi 1999; see also Schinnerer 1999). NGC 3227 ($D = 17.3$ Mpc, group distance; Garcia 1993) is of type 1.2 (Osterbrock 1977) and contains a large amount of molecular gas in its central region (Meixner et al. 1990). It has an ionization cone mapped with HST in the [O III] line emission (Schmitt & Kinney 1996).

NGC 1068 ($D = 14$ Mpc; Bland-Hawthorn et al. 1997) is the archetypical Seyfert 2 galaxy. Antonucci & Miller (1985) observed emission lines widths typical for BLR lines of Seyfert 1's in the polarized optical emission of this galaxy. In addition to bright molecular spiral arms at $r \sim 1$ kpc there is also molecular gas observed at the nuclear region (Jackson et al. 1993, Tacconi et al. 1994, Helfer & Blitz 1995, Tacconi et al. 1997, Baker & Scoville 1998). A prominent ionization cone is traced in the [O III] line emission (Macchetto et al. 1994).

2. OBSERVATIONS AND RESULTS

In both galaxies the ^{12}CO (2-1) line emission was observed in the winter of 1996/1997 using the IRAM millimeter interferometer (PdBI) on the Plateau de Bure, France, in its AB configuration. The five antennas were positioned in three (NGC 3227) and two (NGC 1068) different configurations providing 30 and 20 baselines, respectively. The angular resolution is $\sim 0.6''$ for NGC 3227 and $\sim 0.7''$ for NGC 1068. Further details of the observations will be given in Schinnerer, Eckart, Tacconi (1999) and Schinnerer et al. (1999).

As shown in Fig. 1a and 1b the nuclear ^{12}CO (2-1) emission in both galaxies has a ring-like distribution. Fig. 2 and Fig. 3 show position velocity diagrams taken along or close to the kinematic axes of NGC 3227 and NGC 1068, respectively. The extreme velocities (indicated by arrows) seen for the first time in the molecular line emission of **both** galaxies indicate rising rotation curves towards smallest radial separations and large enclosed masses of $\geq 2 \times 10^7 M_{\odot}$ for NGC 3227 and $\geq 10^8 M_{\odot}$ for NGC 1068 (see caption

of Fig. 2 and Fig. 3). The general gas motion in NGC 3227 can be described by a rotating disk for radii $>1''$. For this region we obtained a rotation curve using the GIPSY routine ROTCUR. For NGC 1068 a lower limit to the rotation velocity at each radius $\leq 12''$ (well within the spiral arms at $r \sim 15''$) was obtained by averaging the extreme measured velocities on opposite sides of the nucleus independent of position angle. In the inner few parsecs the rotation curve was replaced by Keplerian rotation velocities corresponding to the estimated enclosed masses.

3. THE MODELING

The observed position-velocity data cubes were modeled using three dimensional gas orbits and translating the motion along the line-of-sight axis onto the spectral axis. The orbits representing gas motion are not self-intersecting and do not have strong cusps, since these lead to clumping, dissipation of kinetic energy, and therefore result in unstable orbits (e.g. Friedli & Martinet 1993). Under these assumptions two ways to approximate the gas motions in the circumnuclear region are: (a) planar elliptical orbits and (b) tilted circular orbits. In case (a) the elliptical orbits resemble the two main x_1 - and x_2 -families which are present in bar potentials (see review by Sellwood & Wilkinson 1993). At the position of resonances the stars flip from one family to the other, whereas the gas smoothly follows this change. The behavior can be mimicked by ellipses with changing eccentricities and position angles (see for example Fig. 7 in Telesco & Decher 1988). In case (b) the tilted circular orbits form a precessing warp in the gas disk. Such warps are quite common in HI disks in the outer regions of galaxies (see review by Binney 1992), and are also observed in the accretion disks around AGN (e.g. NGC 4258, Miyoshi et al. 1995). We neglect radiative transfer processes assuming that, due to the large nuclear velocity dispersions, the bulk of the molecular gas is not strongly effected by self-absorption.

The model subdivided the disk into many single (circular or elliptical) orbits of molecular gas. For the modeling the inclination, position angle and shape of the rotation curve for each host galaxy were held fixed. Each fitting process was started at large radii and successively extended towards the center. For each case we tried several start set-ups that all converged to similar (best) solutions with mean deviations from the data of less than about 10 km/s and $0.1''$ for each velocity and radius in the pv-diagrams and 10° in the position angle of the mapped structures.

To model the warp we followed the method of Tubbs (1980; see also Quillen et al. 1992). In this approach the warp is produced by a smooth variation of the tilt $\omega(r)$ of each orbit relative to the plane of the galaxy and the precession angle $\alpha(r)$. A torque acting on an orbit with a circular velocity $v_c(r)$ introduces a precession rate $d\alpha/dt \sim \xi v_c/r$. After a time Δt one obtains $\alpha(r) = \xi \Omega \Delta t + \alpha_0$. Here α_0 is a constant, $\Omega = v_c/r$, and ξ is given by the acting torque. We considered for our analysis models with constant $\xi \Delta t$ and assume the molecular gas to be uniformly distributed.

For the bar approach we fitted the orbital eccentricity $\epsilon(r) = b(r)/a(r)$ (b is the minor

axis, a is the major axis) and the position angle $PA_{ellipse}(r)$ as curves varying smoothly with radius under the constraint that the orbits do not overlap with each other. The orbits lie in a plane and resemble velocity and density distributions similar to the bar models of Athanassoula (1992).

The fitting was done on host galaxy kinematic major and minor axes pv-diagrams and checked on the overall intensity map and the velocity field. Here we concentrate on the central few arcseconds and present the results for the two galaxies by first describing the essential properties of the pv-diagrams and then giving an outline of the best bar and warp models.

3.1. NGC 3227

For NGC 3227 two representative pv-diagrams are shown in Fig. 2. They are taken along the major kinematic axis (PA 158°) and a position angle of PA 40° consistent with spatial extent of the nuclear emission. Along the major axis the drop of the rotational velocity can be seen down to $r \sim 0.5''$. For smaller radii an apparent counter rotation is observed between $0.2'' \leq r \leq 0.5''$. For even smaller radii a second flip back to the original sense of rotation is detected. These changes in rotation form a S-shape in the inner $1''$ of the pv-diagram. At PA 40° (close to the kinematic minor axis) a similar behavior is seen with the exception that the change in the sense of rotation is already occurring at $r \sim 0.6''$. East of the dynamical nucleus this pv-diagram clearly shows an enhancement of emission which is poorly reproduced by the models, since it is not axisymmetric.

The bar approach: Fig. 2 shows that we are not able to account for the observed amount of counter rotation along the kinematic major axis and especially along PA 40° close to the kinematic minor axis. Also, in both pv-diagrams the S-shape in the inner $1''$ is not all reproduced. Combined with the fact that high resolution NIR observations (Schinnerer, Eckart, Tacconi 1999, Schinnerer 1999) show no evidence for a nuclear bar, this suggests that the observed structure and *kinematics* of the inner $1''$ are not well represented by motion of gas in a *nuclear* bar potential. However, the circumnuclear ring ($r \approx 1.5''$) may well be due to an ILR of an outer structure.

The warp approach: Fig. 2 shows the fits of the best warp model to both pv-diagrams. The model reproduces the observed S-shaped changes in the rotational sense in both pv-diagrams, as well as the observed intensity distribution in the inner $1''$ (Fig. 1a). This success in reproducing *both* the kinematics and source structure suggests that a warped disk, rather than an inner bar, is a more realistic description of the molecular gas in the central 70 pc of this galaxy.

3.2. NGC 1068

The kinematic major axis of NGC 1068 lies along a position angle of $PA \sim 110^\circ$; and the position-velocity cut along this PA is remarkably symmetric (Fig. 3). The large scale disk emission is observed at radii $\geq 2''$. A large velocity dispersion, which even rises above the rotational velocity, is seen at $r = 1''$. Finally we also observe emission at the systemic velocity which is detected at radii $\leq 0.9''$ and in a ridge which connects the two high dispersion points at $r = 1''$.

The bar approach: The best bar model reproduces the overall shape of the pv-diagram. However, Fig. 3 shows that although the high velocity dispersion at $1''$ can be fitted, this model fails to produce the rise in velocity relative to the neighboring disk emission and the emission ridge. The bar model requires highly elliptical orbits inside the ring thus making the interpretation as an ILR of the 2 kpc stellar NIR bar (Scoville et al. 1988) very unlikely, since it is expected that the orbits become more circular inside the ILR (e.g. Athanassoula 1992). We regard the bar model as a satisfying but not good fit to the data - especially given the fact that the nuclear stellar cluster as mapped by Thatte et al. (1997) shows no indication for separate bar-like structure that might induce the highly elliptical orbits.

The warp approach: The best warp model is displayed in Fig. 3. All observed kinematic features are reproduced by this model: the disk emission, the high dispersion plus rise in velocity, the emission at the systemic velocity as well as the ridge between the high dispersion peaks. We thus favor a warped disk over a nuclear bar distribution to describe the gas distribution and motion in NGC 1068 at $r \leq 1.5''$.

In this model the sudden increase in observed projected velocity as well as the high velocity dispersion at $1''$ is due to molecular gas forming an edge-on disk at this radial distance (see Fig. 4). Such a disk is in agreement with the observed orientation of the NIR/MIR polarization vectors (Young et al. 1996, Lumsden et al. 1999) and the extinction band across the nuclear region (Catchpole & Boksenberg 1997). The three-dimensional geometry of the warp also naturally provides a cavity for the ionization cone in consistency with the observed orientation (see Fig. 4).

4. CONSEQUENCES AND IMPLICATIONS

The warp model provides the better fit to the kinematics of the molecular gas in the circumnuclear regions of both studied Seyfert galaxies (as outlined above). The bar model might work if one allows for high streaming motions providing further velocity modulation in the pv-diagrams. This would, however, favor stronger nuclear bars which are **not** indicated by high resolution NIR observations (Thatte et al. 1997, Schinnerer, Eckart, Tacconi 1999, Schinnerer 1999).

The fits to the data imply that even at radii as small as $r \sim 75$ pc the gas stays in a thin disk with low velocity dispersion (<30 km/s) while the stars show an almost spherical

distribution at these distances. The magnitude of the torque estimated from the warp model (Sparke 1996) implies that the most likely cause for such a warp of this thin gas layer is a torque induced by the gas pressure of the ionization cones in both galaxies. An important future test will be a comparison of molecular gas kinematics in galaxies with and without ionization cones. Alternatively, as a transient phenomenon, complexes of molecular clouds which do not participate in the overall gas motion can also induce a torque on the gas disk.

Since the observed features are symmetric with respect to the dynamical center, a scenario in which the source structure is dominated by randomly distributed molecular cloud complexes also appears to be very unlikely. Our results suggest that future theoretical studies of molecular gas dynamics in the circumnuclear regions *will require* 3 dimensional modeling.

The molecular gas being distributed in a thin, warped disk can have important consequences for AGN obscuration (and the structure and evolution of the NLR). Such a disk when viewed edge-on - as in the case of NGC 1068 - can effectively hide the Seyfert nucleus from direct view. This conclusion is supported by other recent studies of samples of Seyfert galaxies which find that the molecular gas and dust at distances of about 100 pc can play a significant role in the classification of Seyfert galaxies (Malkan et al. 1998, Cameron et al. 1993).

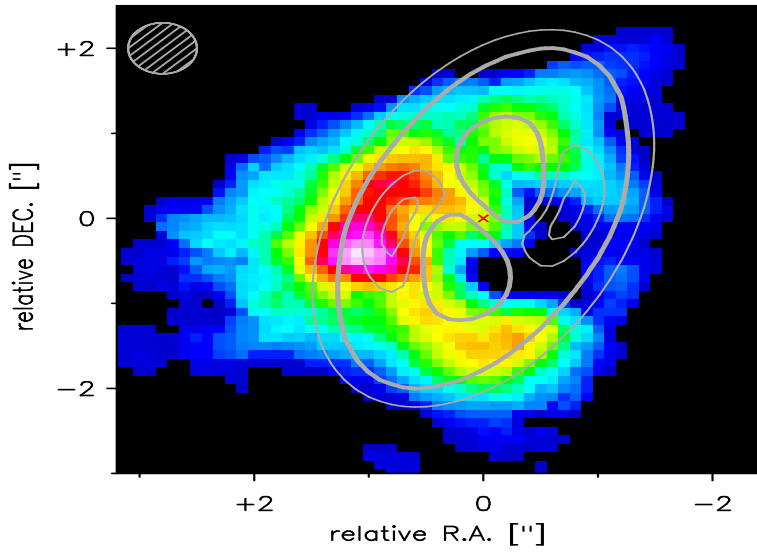
Our results also indicate that that nuclear bars are not necessarily the primary fueling mechanism for AGN activity, since we can describe the gas distribution very well by a uniform warped disk. This is in agreement with data presented by Regan & Mulchaey (1999) who did not find evidence for strong bars in their Seyfert sample. As the ionization cone is likely to cause the warp this would then also provide the connection between the AGN and the inner part of its host galaxy. Supported by these statistical findings our results imply that the AGN and its host galaxy are not discrete systems but are naturally linked to each other.

We like to thank the IRAM Plateau de Bure staff for carrying out the observations and the staff at IRAM Grenoble, especially R. Neri and D. Downes, for their help during the data reduction. For fruitful and stimulating discussions we thank A. Baker, D. Downes, P. Englmaier, R. Genzel, O. Gerhard, A. Quillen, N. Scoville and L. Sparke.

REFERENCES

- Antonucci, R.R.J., Miller, J.S., 1985, *Ap. J.*, 297, 621.
- Athanassoula, E., 1992, *M.N.R.A.S.*, 259, 345.
- Baker, A.J, Scoville, N.Z., 1998, *Proceedings of IAU Symposium 184*, ed. Y. Sofue (Dordrecht:Kluwer), 221
- Binney, J., 1992, *Ann.Rev.Astr.Ap.*, 30, 51.
- Bland-Hawthorn, J., Gallimore, J.F., Tacconi, L., Brinks, E., Baum, S.A., Antonucci, R.R.J., Cecil, G.N., 1997, *Ap. & S.S.*, 248, 9.
- Cameron, M., Storey, J.W.V., Rotaciuc, V., Genzel, R., Verstraete, L., Drapatz, S., Siebenmorgen, R., Lee, T.J., 1993, *ApJ419136*
- Catchpole, R.M., Boksenberg, A., 1997, *Ap. & S.S.*, 248, 79.
- Friedli, D., Martinet, L., 1993, *Astron. Astrophys.*, 277, 27.
- Garcia, A.M., 1993, *Astron. Astrophys. Suppl.*, 100, 47.
- Greenhill, L.J., Gwinn, C.R., 1997, *Ap. & S.S.*, 248, 261.
- Helfer, T.T., Blitz, L., 1995, *Ap. J.*, 450, 90.
- Jackson, J.M., Paglione, T.A.D., Ishizuki, S., Nguyen-Q-Rieu, 1993, *Ap. J. (Letters)*, 418, L13.
- Lumsden, S.L., Moore, T.J.T., Smith, C., Fujiyoshi, T., Bland-Hawthorn, J., Ward, M.J., 1999, *M.N.R.A.S.*, 303, 209.
- Macchetto, F., Capetti, A., Sparks, W.B., Axon, D.J., Boksenberg, A., 1994, *Ap. J. (Letters)*, 435, L18.
- Malkan, M.A., Gorjian, V., Tam, R., 1998, *Ap. J. Supp.*, 117, 25.
- Meixner, M., Puchalsky, R., Blitz, L., Wright, M., Heckman, T., 1990, *Ap. J.*, 354, 158.
- Miyoshi, M., Moran, J., Herrnstein, J., Greenhill, L., Nakai, N., Diamond, P., Inoue, M., 1995, *Nature*, 373, 127
- Peterson, B., 1997, *An Introduction to Active Galactic Nuclei*, Cambridge, Cambridge Univ. Press
- Quillen, A.C., De Zeeuw, P.T., Phinney, E.S., Phillips, T.G., 1992, *Ap. J.*, 391, 121.
- Osterbrock, D.E., 1977, *Ap. J.*, 215, 733.
- Regan, M.W., Mulchaey, J.S., 1999, *A. J.*, in press, .
- Salamanca, I. et al., 1994, *Astron. Astrophys.*, 282, 742.
- Schinnerer, E., Eckart, A., Tacconi, L.J., Genzel, R., Downes, D. 1999, in preparation
- Schinnerer, E., Eckart, A., Tacconi, L.J., 1999, in preparation
- Schinnerer, E., 1999 Ph.D. thesis, Ludwig-Maximilians-Universität, München, Germany

- Schmitt, H.R., Kinney, A.L., 1996, ApJ463498
- Scoville, N.Z., Matthews, K., Carico, D.P., Sanders, D.B., 1988, Ap. J. (Letters), 327, L61.
- Sellwood, J.A., Wilkinson, A., 1993, Rep. Prog. Phys., 56, 173
- Sparke, L.S., 1996, Ap. J., 473, 810.
- Tacconi, L.J., Gallimore, J.F., Genzel, R., Schinnerer, E., Downes, D., 1997, Ap. & S.S., 248, 59.
- Tacconi, L.J., Genzel, R., Blietz, M., Cameron, M., Harris, A.I., Madden, S., 1994, Ap. J. (Letters), 426, L77.
- Telesco, C.M., Decher, R., 1988, Ap. J., 334, 573.
- Thatte, N., Quirrenbach, A., Genzel, R., Maiolino, R., Tecza, M., 1997, Ap. J., 490, 238.
- Tubbs, A.D., 1980, Ap. J., 241, 969.
- Young, S., Packham, C., Hough, J.H., und Efsathiou, A., 1996, M.N.R.A.S., 283, L1.



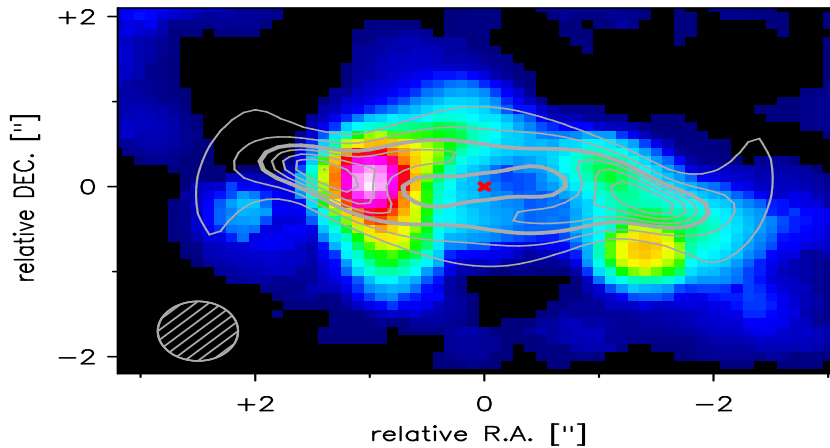


Fig. 1.— Intensity maps of the ^{12}CO (2-1) line emission in NGC 3227 (a) and NGC 1068 (b) in colour. In both galaxies the ^{12}CO (2-1) emission is distributed in ring-like features with radii ~ 150 pc. In both sources nuclear line emission is clearly detected ($> 3\sigma$). The contours show the intensity maps of the best warp models. Contour levels for NGC 3227 (a) are 40 %, 65 % (thick), 80 %, 90 % and for NGC 1068 (b) 30 %, 45 %, 60 % (thick), 70 %, 80 %, 90 % of the peak intensity. The thick contour lines outline the circumference of the overall structures and their local minima. The red crosses mark the positions of the fitted dynamical centers.

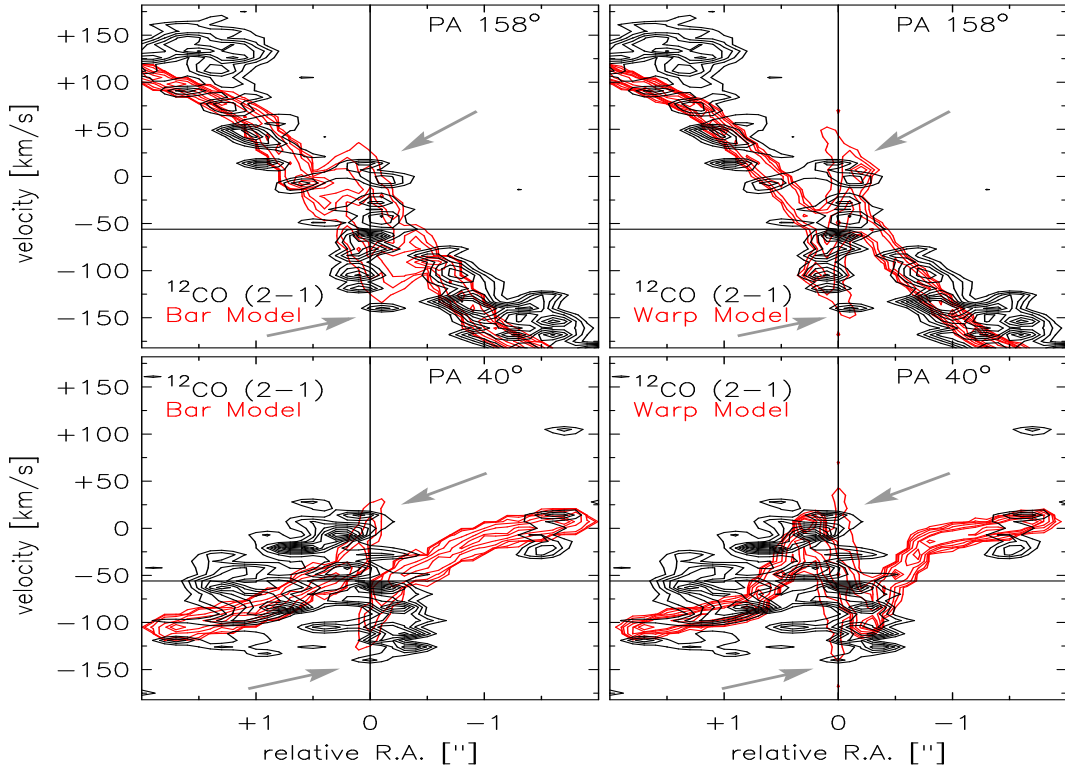


Fig. 2.— pv-diagrams in NGC 3227. Top: The data (black contours) along the kinematic major axis (PA 158°) are shown together with the results (red contours) of the bar model (left) and the warp model (right). Similarly the data and the results along PA 40° are shown at the bottom. In the pv-diagram at a resolution of $0.6''$ the lowest contour corresponds to 3σ , with $1\sigma = 6.2$ mJy/beam at a spectral resolution of 7 km/s. To highlight the complex velocity behavior the data is shown at $0.3''$ (higher than the effective resolution) close to the resolution of the model ($\sim 0.2''$). For the first time seen in the molecular gas emission the data shows a rising rotation curve towards smaller radii with the extreme velocities (indicated by arrows) at radial separations of $\approx 0.15''$ (13 pc) indicating an enclosed mass of $\geq 2 \times 10^7 M_\odot$, not correcting for inclination effects. This value is consistent with $\sim 10^8 M_\odot$ estimated from H β -reverberations mapping by Salamanca et al. (1994).

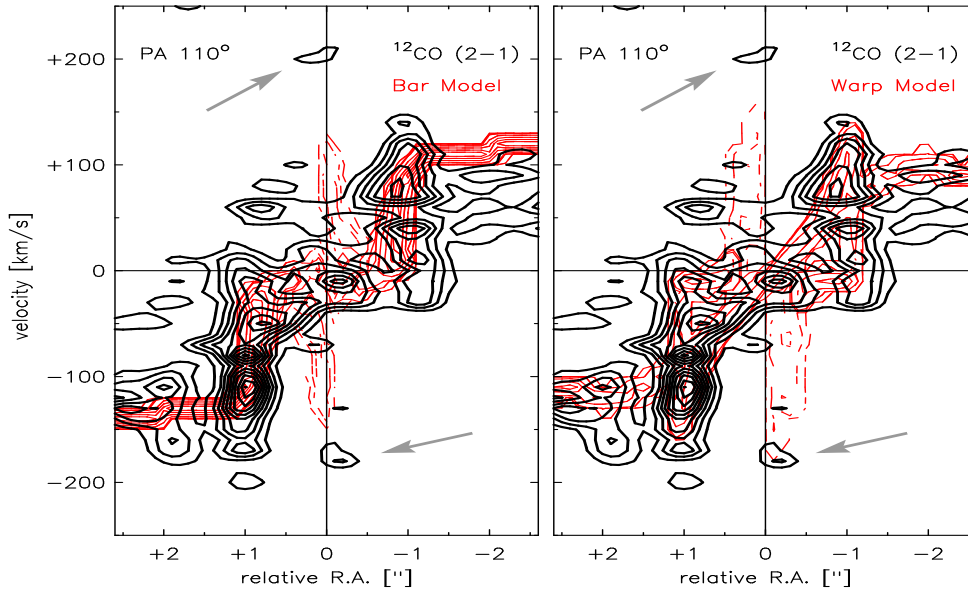


Fig. 3.— pv-diagrams in NGC 1068: The data (black contours) along PA 110° are shown together with the results (red solid contours) of the bar model (left) and the warp model (right). In the pv-diagram at a resolution of $0.7''$ the lowest contour corresponds to 3σ , with $1\sigma = 11$ mJy/beam at a spectral resolution of 10 km/s. To highlight the complex velocity behavior the data is shown at $0.4''$ (higher than the effective resolution) close to the resolution of the model ($\sim 0.2''$). As in NGC 3227 the velocity data at radial separations of $\approx 0.18''$ (13 pc) (indicated by arrows) indicates an enclosed mass of $\gtrsim 10^8 M_\odot$, not correcting for inclination effects. Models resulting from a rotation curve including the effect of such a central mass are shown in solid and dashed red contours. Including a possible contribution from a compact nuclear stellar cluster this value is consistent with a black hole mass of $1.7 \times 10^7 M_\odot$ estimated from nuclear H_2O -maser emissions by Greenhill & Gwinn (1997).

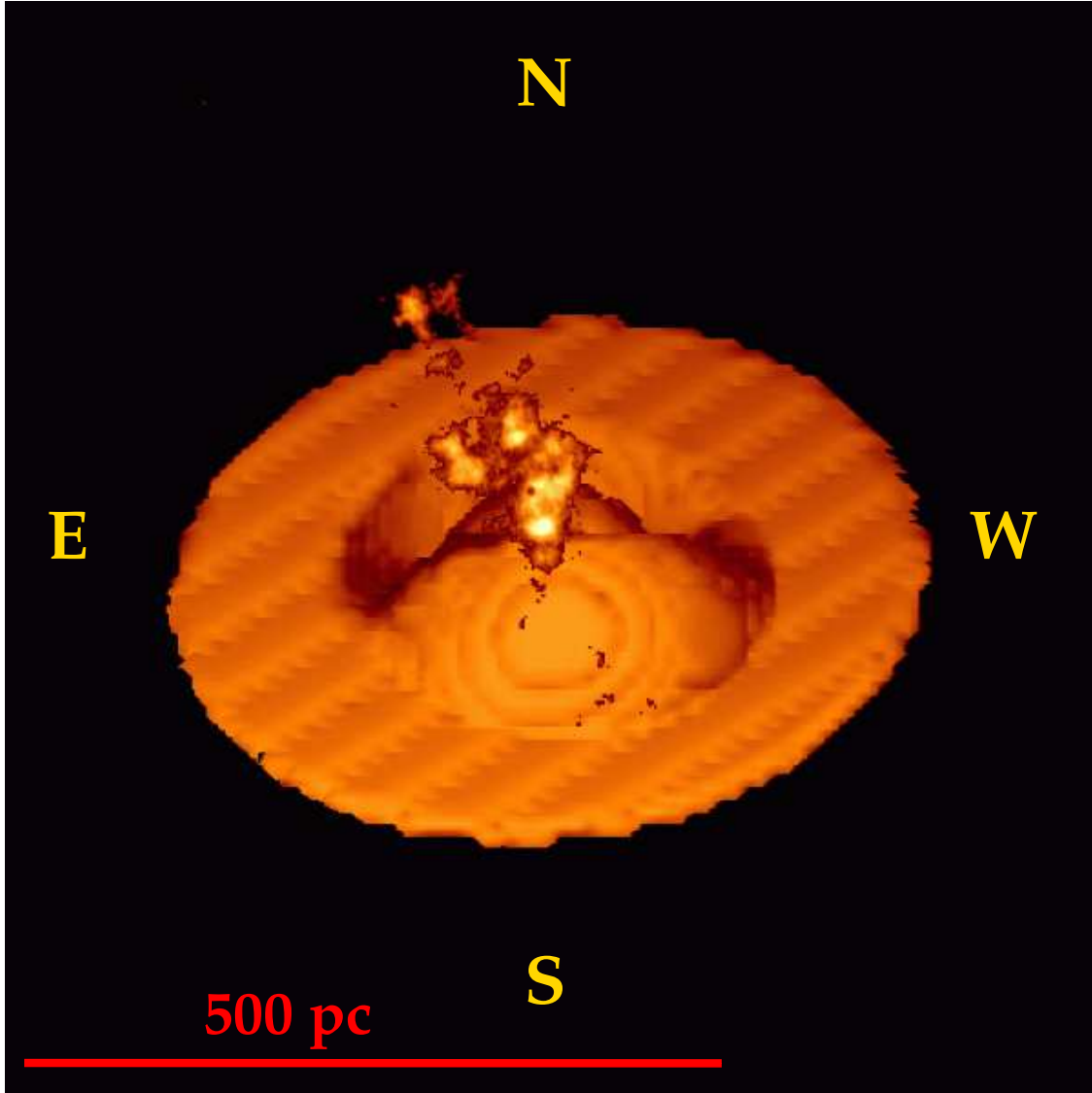


Fig. 4.— Spatial geometry of the warp model of NGC 1068. Bright colors of the warped disk indicate sections that are closer to the observer, darker colors those further away. The ionization cone as seen in the [O III] line emission of Macchetto et al. (1994) is displayed as the brightest structure. The three-dimensional geometry of the warp naturally provides a cavity for the ionization cone in consistency with the observed orientation.